Communication

A Single-Turn Stacked Spiral Antenna With Ultrawide Bandwidth and Compact Size

Long Zhang, Ning Luo, Yuhang Sun, Yejun He, Sai-Wai Wong, Peng Chu, Chunxu Mao, and Steven Gao

***Abstract*— An ultrawideband stacked single-turn spiral antenna with an integrated feeding structure is presented in this communication. The proposed antenna consists of two stacked planar single-turn Archimedean spirals which are wound in orthogonal directions. By connecting these two stacked spirals through two vertical posts, the traveling-wave current path is lengthened and, hence, the operating frequency of Mode 1 is decreased. To reduce the feeding complexity, an integrated tapered microstrip line is used to feed the spiral, which also acts an impedance transformer. It is demonstrated that the proposed antenna can operate across 0.29–5 GHz with $|S_{11}| < -10$ dB and 0.75–3.64 GHz with axial ratio (AR) <3 dB. Compared with the single-turn Archimedean spiral with the same radius, the impedance and AR bandwidth of the proposed antenna are enhanced from 5:1 to 17:1 and from 1.6:1 to 4.9:1, respectively, showing that the proposed antenna can be a good candidate for ultrawideband applications.**

***Index Terms*— Archimedean spiral antenna, stacked spiral, wideband antenna.**

I. Introduction

The Archimedean spiral antennas are favorable candidates for various commercial devices attributed to their broad bandwidth [1]. However, traditional Archimedean spirals have two common issues, which hinder their potential applications. The first one is the need of a complex feeding balun, which transforms the high input impedance of the spiral to 50 Ω [2]. The other one is the large diameter, which is always beyond one wavelength when several octave bandwidths are demanded [3].

To simplify the feeding structure of the spiral antennas, several planar impedance transformers were proposed. A tapered stripline impedance transformer was proposed in [4] and [5]. But the influence of the stripline on the axial ratio (AR) was not investigated. Two microstrip line feeds printed on the opposite side of the spiral were presented in [6]. However, two coaxial cables are needed to connect the microstrip lines and a 90° hybrid is required. In [7], an integrated impedance transformer by employing tapered transmission lines was presented to feed a four-arm Archimedean spiral antenna. But an additional beam-forming network is needed to connect the four SMA connectors. An integrated parallel-plane transmission line was utilized to feed an equiangular spiral antenna [8]. But the AR is larger than 3 dB across the whole frequency range. A spiral antenna with external coplanar waveguide feeding structure was presented in [9]. However, a consecutive phase shift of 90° is required for the four external feeding ports, which increases the complexity of the feeding structure.

In order to broaden the bandwidth of the spiral antenna without increasing its radius, a stacked four-turn spiral antenna was proposed in [10]. However, each separated spiral is of inherent ultrawide bandwidth and considerable diameter size. Moreover, the AR of the stacked spiral is deteriorated at high band. Thus, this is not an efficient way to increase the bandwidth without deteriorating the performance of the spirals. In addition, the practical impedance matching method was not addressed. In [11], the current path of an Archimedean spiral was elongated by extending the two arms around a cylinder and four resistors were loaded to improve the impedance bandwidth. However, a vertical feeding balun was required to feed the spirals. In [12], parasitic metallic posts were incorporated to improve the bandwidth of an equiangular spiral. Nevertheless, the measured AR was around 5 dB within the band of interest. In [13], the bandwidth of the spiral antennas was greatly improved by connecting the arms of adjacent spirals in a ring array. A circularly symmetric high-impedance surface (HIS) was utilized as a ground plane to improve the bandwidth of the spirals, which yet increased the overall antenna size [14].

In this communication, a circularly polarized (CP) stacked spiral antenna with small diameter and improved bandwidth is presented. By integrating a planar feeding structure, a two-step impedance matching method is realized to improve the bandwidth performance. To further improve the bandwidth of a single-turn spiral antenna, two stacked spiral antennas with orthogonal polarizations are vertically connected through two copper posts. By doing this, the path of the traveling-wave current can be lengthened effectively without increasing its radius, which reduces the operating frequency of Mode 1 [15]. As a consequence, the lower limit of the operating band can be greatly decreased, while the upper limit remains unchanged, resulting in a broader bandwidth. Compared with traditional spiral antennas, the proposed antenna features enhanced bandwidth and compact size and, thus, is suitable for ultrawideband CP applications.

II. Antenna Configuration and Operating Principles

A. Antenna Configuration and Impedance Matching

The geometry of the proposed stacked spiral antenna is shown in Fig. 1, which is mainly composed of three parts, the lower spiral, the upper spiral, and two copper posts. As shown in Fig. 1, the lower spiral is printed on the top side of substrate 2 (FR4 with a dielectric constant of 4.4 and a loss tangent of 0.02), where a 75 Ω RF resistor

Manuscript received August 21, 2019; revised July 10, 2020; accepted July 26, 2020. Date of publication August 19, 2020; date of current version March 3, 2021. This work was supported in part by the National Natural Science Foundation of China under Grant 61801299, in part by the Natural Science Foundation of Guangdong Province under Grant 2020A1515011037, in part by the Exchange Program for Taiwan Young Scientists under Grant RW2019TW001, and in part by the Shenzhen Science and Technology Program under Grant GJHZ20180418190529516 and Grant JSGG20180507183-215520. *(Corresponding author: Yejun He.)*

Long Zhang, Ning Luo, Yuhang Sun, Yejun He, and Sai-Wai Wong are with the College of Electronics and Information Engineering, Shenzhen University, Shenzhen 518060, China (e-mail: long.zhang@szu.edu.cn; heyejun@126.com).

Peng Chu is with the College of Electronic and Optical Engineering, Nanjing University of Posts and Telecommunications, Nanjing 210023, China.

Chunxu Mao is with the 5G Innovation Centre (5GIC), Institute for Communication Systems (ICS), University of Surrey, Guildford GU2 7XH, U.K.

Steven Gao is with the School of Engineering and Digital Arts, University of Kent, Canterbury CT2 7NT, U.K. (e-mail: s.gao@kent.ac.uk).

Color versions of one or more of the figures in this communication are available online at https://ieeexplore.ieee.org.

Digital Object Identifier 10.1109/TAP.2020.3016503

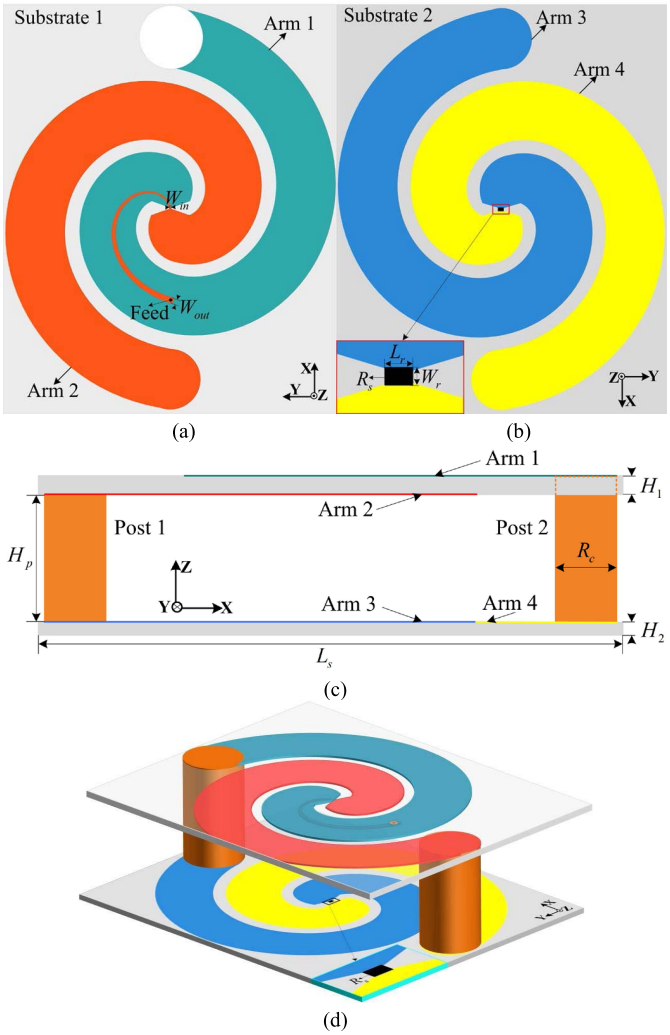

Fig. 1. Configuration of the proposed antenna. (a) Top view of the upper spiral. (b) Top view of the lower spiral. (c) Side view of the proposed antenna. (d) Perspective view of the proposed antenna.

TABLE I
ANTENNA DIMENSIONS (mm)

Parameter	R_C	H_P	H_1	H_2	L_r	L_S	W_S	W_{in}	W_{out}	W_r
Value	20	17.5	1	0.6	0.6	129	105	0.5	1.88	0.7

[R_S in Fig. 1(b)] is loaded at the center of the lower spiral. The upper spiral is printed on both side of the substrate 1 (FR4). As shown in Fig. 1(a), a tapered microstrip line connecting to the arm 2 is printed on the bottom layer of substrate 1, while the arm 1 printed on the top layer acts as the ground plane for the tapered microstrip line. In order to elongate the spiral current path, the ends of the two spiral arms are connected by two copper posts, as shown in Fig. 1(c). Table I summarizes the detailed geometry dimensions of the proposed stacked spiral antenna, where L_S and W_S represent the length and width of the substrate, respectively.

Normally, a self-complementary two-arm spiral antenna has a relatively high input impedance (about 188 Ω for a freestanding spiral), which is hard to be matched by a 50 Ω microstrip line directly. For satisfactory impedance matching, it is necessary to decrease the antenna input impedance to a lower value at first. Increasing the spiral's metal to slot ratio (MSR) is an effective way to reduce the input impedance (for self-complementary antenna

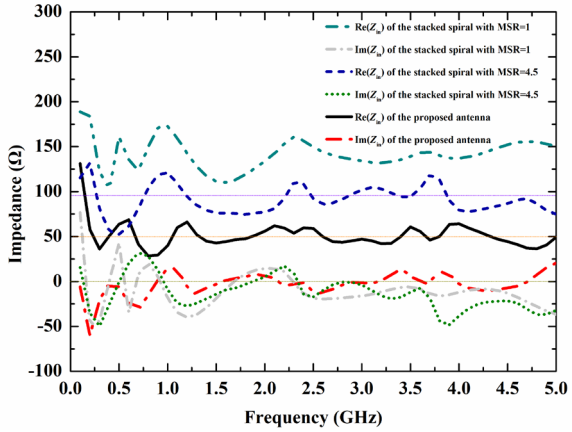

Fig. 2. Variation of input impedance during the two-step impedance matching procedure.

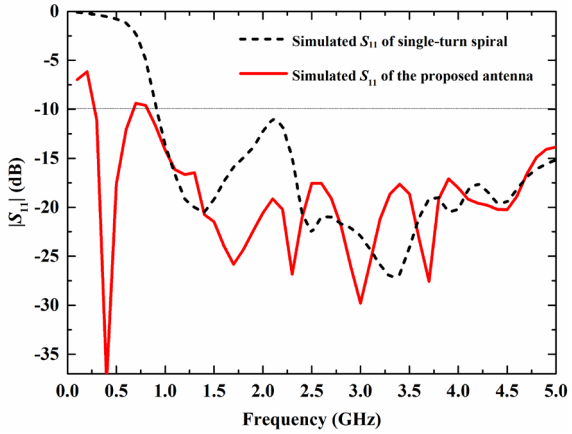

Fig. 3. Comparison of the simulated $|S_{11}|$ between the single-turn spiral and the proposed antenna.

MSR = 1) [6]. The specific impedance value for different MSRs can be evaluated by the formula provided in [16]. By choosing an MSR of 4.5, the input impedance of the stacked spiral antenna can be reduced to 90 Ω. A tapered microstrip line is then used to feed the antenna, which transforms the input impedance from 90 to 50 Ω. Fig. 2 shows the two-step impedance matching procedure.

The simulated reflection coefficients of the proposed stacked spiral antenna and the single-turn spiral with the same radius are depicted in Fig. 3. As shown, excellent impedance matching is realized in the frequency range from 0.29 to more than 5 GHz. It should be noticed that the lower cutoff frequency of the single-turn spiral is greatly decreased from 1 to 0.29 GHz by stacking two single-turn spirals together.

B. Mechanism of AR Bandwidth Improvement

It is well-known that the AR bandwidth will be severely deteriorated when the spiral is designed with single-turn arms due to the large growth rate and reflection at the termination of the spiral arms. To improve the AR bandwidth of the single-turn spiral, two spirals with orthogonal polarizations are stacked and connected by two copper posts. With this arrangement, the electric current can flow from the upper spiral to the lower spiral, which avoids the current reflection at the end of upper spiral arm. The lengthened traveling-wave current path enables the proposed antenna operate in Mode 1 at a much lower frequency. On the contrary, due to the reflection at the termination of the spiral arm, the single-turn spiral operates

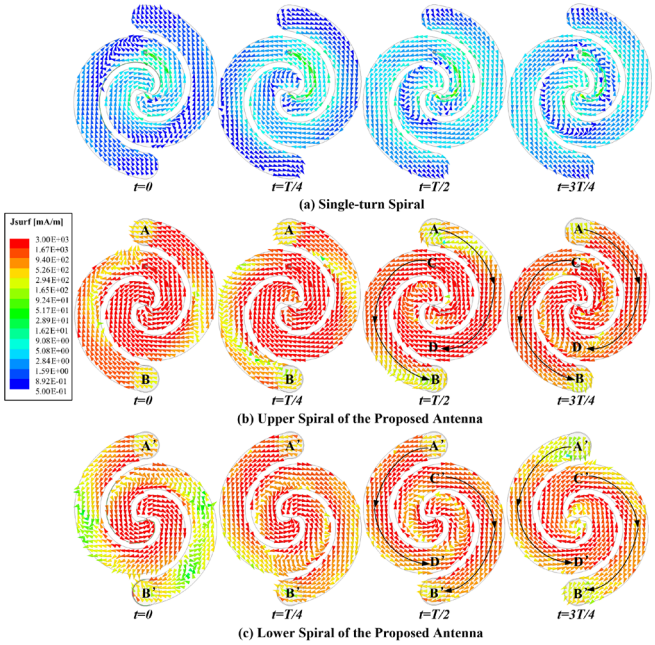

Fig. 4. Simulated current distribution on the single-turn spiral and the proposed antenna at 1 GHz. (a) Current distribution on the single-turn spiral. (b) Current distribution on the upper spiral. (c) Current distribution on the lower spiral.

in Mode 1 at higher frequency. Consequently, the low-end cutoff frequency of the proposed spiral antenna is greatly reduced, while the high-end cutoff frequency remains the same as the single-turn spiral. The operating frequency of Mode 1 can also be reduced by increasing the number of spiral turns, but this will yield larger antenna diameter.

Fig. 4 compares the current distribution at 1 GHz between the single-turn spiral and the proposed antenna. As shown, the magnitude of surface current along the proposed antenna is much larger than that of the single-turn spiral due to the lengthened current path. Moreover, as shown in Fig. 4(b) and (c), the directions of surface currents along curves A′D′ and C′B′ are the same as that along curves CB and AD, respectively. Notice that curves A′D′ and C′B′ are neighboring arms to the curves CB and AD, respectively, due to the stacked configuration. Therefore, Mode 1 radiation will occur along these curves according to the radiating ring theory [1]. Since the active region of Mode 1 is greatly increased due to the lengthened traveling-wave current along the lower spiral, the proposed antenna can operate in Mode 1 at much lower frequency than the single-turn spiral. The comparison of the AR bandwidth between the single-turn spiral and the proposed antenna is demonstrated in Fig. 5. From Fig. 5, it is noticed that the 3 dB AR bandwidth is greatly improved by stacking two single-turn spirals together since the low-frequency limit shifts from 2.25 to 0.67 GHz.

It is worth pointing out that an RF resistor (R_S) is placed at the center of the lower spiral to absorb the residual current, which helps improve the bandwidth performance. Without this resistor, the impedance matching and AR performance will be degraded due to the reflections from the lower spiral and vertical posts. Although it absorbs the residual power and reduces the radiation efficiency at low frequencies, the lengthened traveling-wave current still improve the radiation performance. The resistance value of this resistor should be close to the input impedance of the single-turn spiral with MSR of 4.5 (90 Ω). A 75 Ω resistor is finally chosen due to the availability of stock.

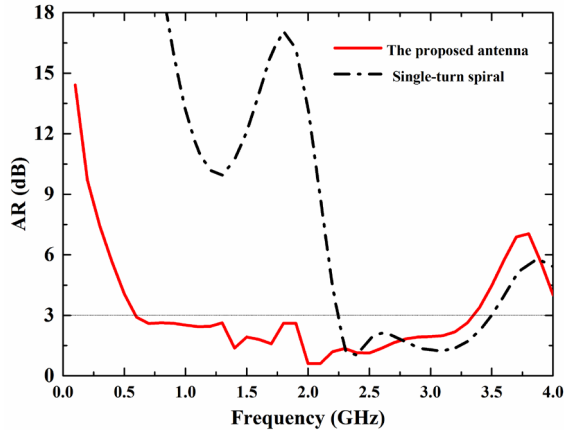

Fig. 5. Comparison of the AR between the single-turn spiral and the proposed antenna.

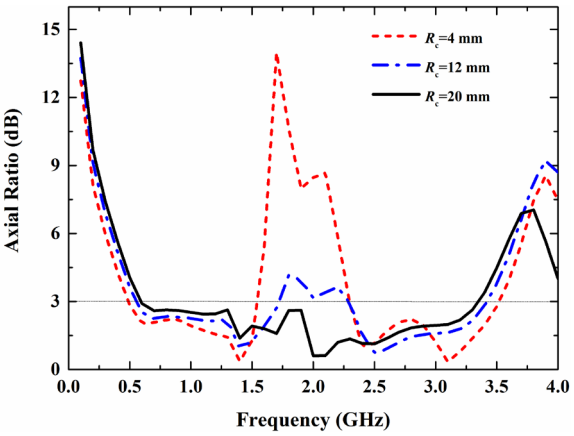

Fig. 6. Effect of copper posts diameter on the AR.

C. Investigation of Copper Posts Connection

From simulation, it is found that the diameter of the copper post (R_C) affects the antenna performance to a great extent. The effect of R_C on the AR is shown in Fig. 6. As shown, the diameter R_C has considerable influences on the AR in the frequency range from 1.5 to 2.4 GHz. When the diameter of the post is smaller than 20 mm, the AR degrades in the frequency range from 1.5 to 2.4 GHz. To investigate this phenomenon, the current distribution on the proposed antenna with different post diameters at 2.1 GHz is depicted in Fig. 7. Attributed to the skin effect of copper, the electric current is mainly concentrated on the surface of the two posts when it is guided to the lower spiral, as indicated in Fig. 7. Notice that the current on the smaller post is uniform around the post surface; it flows to the lower spiral concentrating around the post (see Area1 and Area2). This focused current then spreads radially around the post, which truncates the spiral current. On the contrary, when the diameter of the post is close to the trace width of the spiral, the guided current along the post is not diffused. Instead, the guided current flows inwardly along the lower spiral [see the arrows in Fig. 7(b)], which lengthens the traveling-wave current. Similar phenomena are observed at other frequencies in this frequency range. Therefore, by increasing the diameter of the post to the width of spiral arms, the proposed antenna achieves ultrawide AR bandwidth.

D. Effect of the Tapered Microstrip Line

As aforementioned, a tapered microstrip line is integrated into the antenna acting as a feed line and an impedance transformer.

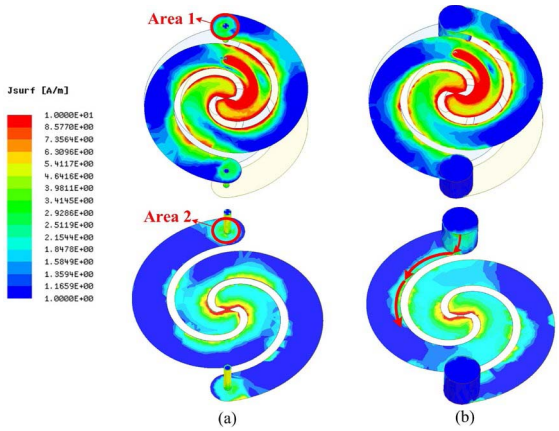

Fig. 7. Current distribution of the proposed antenna with different post diameter at 2.1 GHz. (a) Current distribution with smaller posts. (b) Current distribution with bigger posts.

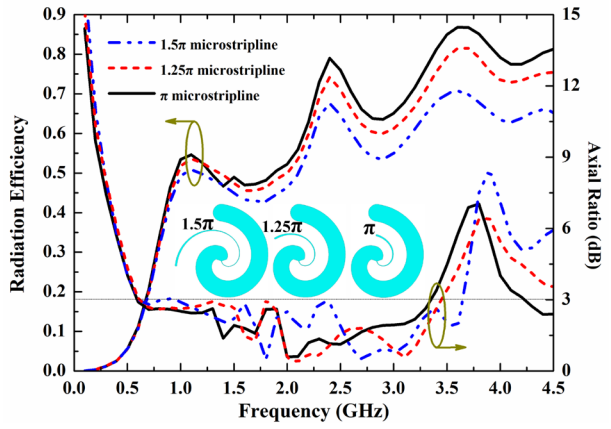

Fig. 8. Effect of microstrip line length on the radiation efficiency and AR.

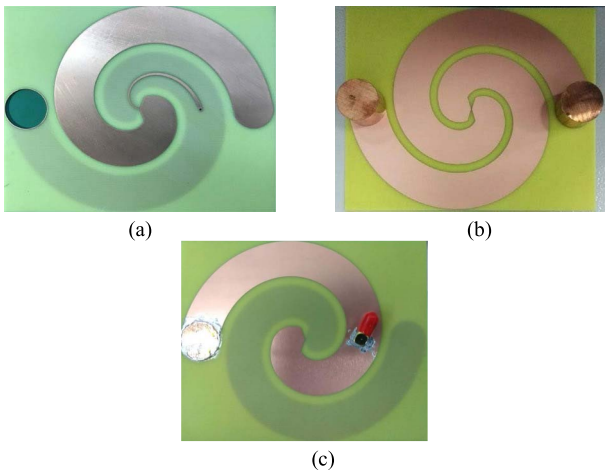

Fig. 9. Fabricated prototype of the proposed antenna. (a) Upper spiral. (b) Lower spiral. (c) Proposed antenna with an SMA connector.

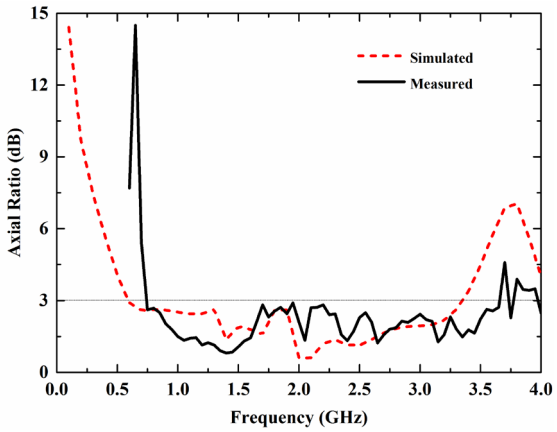

Fig. 10. Simulated and measured AR of the proposed antenna.

To mitigate the radiation of the microstrip line and the coupling between the microstrip line and the spiral arm, the width of microstrip line is designed much smaller than the width of spiral arms. Specifically, the minimum width (W_{in}) and maximum width (W_{out}) of the microstrip line are 0.5 and 1.88 mm, respectively. Hence, the maximum ratio of the width of microstrip line to spiral arm is 1:10.5, which is small enough to minimize the radiation and coupling effect caused by the microstrip line. The utilization of single-turn spiral also alleviates the radiation of the microstrip line, because the smaller number of turns brings larger spiral arm width when the antenna size keeps unchanged.

In addition, the length of the tapered microstrip line also affects the antenna performance. Fig. 8 shows the effect of microstrip line length (represented by different rotation angles π, 1.25π, and 1.5π) on the AR and radiation efficiency. As shown, the length of microstrip line has certain influence on the AR, but the AR bandwidth varies slightly. The increase of the microstrip line length degrades the radiation efficiency notably, especially at the high end of the frequency range. This can be explained by the increased radiation loss and insertion loss of the microstrip line when its length increases. To acquire better antenna performance, a microstrip line with the length of half turn (π) is finally selected.

III. Results and Discussion

Fig. 9 shows the fabricated antenna. As shown, an SMA connector is soldered onto the upper spiral with its inner conductor connected to the tapered microstrip line, and the outer conductor connected to Arm 1 for measurement purpose.

The simulated and measured ARs are presented in Fig. 10. The simulation results are obtained by ANSYS HFSS. As shown, the simulated 3 dB AR bandwidth of the proposed antenna is from 0.67 to 3.35 GHz (5:1), while the measured 3 dB AR bandwidth is from 0.75 to 3.64 GHz (4.87:1). The discrepancy between the measurement and simulation ARs is attributed to the fabrication and measurement errors. The assembly of the stacked spiral, especially the soldering of the copper posts will affect the antenna performance to some extent. Compared with the single-turn spiral, the AR bandwidth of the proposed antenna is improved by more than threefold.

The simulated and measured $|S_{11}|$ of the proposed antenna are depicted in Fig. 11. It is observed that the measured impedance bandwidth is from 0.29 to more than 5 GHz (>17:1), which is also three times larger than the impedance bandwidth of the single-turn spiral. Considering the impedance bandwidth and 3 dB AR bandwidth comprehensively, the proposed antenna can achieve an overlapped bandwidth from 0.75 to 3.64 GHz (4.87:1), while the single-turn spiral antenna can only operate from 2.25 to 3.5 GHz (1.55:1).

Fig. 12 shows the simulated and measured realized gains and radiation efficiencies of the proposed stacked antenna. The measured and simulated realized peak gains are 7.1 and 7.6 dBi, respectively. The simulated and measured radiation efficiencies are also presented in Fig. 12. It is worth mentioning that the measured radiation efficiency is obtained by calculating the ratio of the measured gain to directivity. As shown, the maximum measured radiation efficiency is

TABLE II

PERFORMANCE COMPARISON BETWEEN THE PROPOSED STACKED ANTENNA AND OTHER REPORTED SPIRAL ANTENNAS

Ref	AR (GHz)	S11<-10 dB (GHz)	Reflector	Gain (dBic)	Feeding complexity	Dimension (mm^3) (electrical dimensions at the lowest frequency)	Number of turns	Number of arms
[7]	0.8-3 (3.75:1)	0.5-5 (10:1)	No	0-5.8	Complex	130*130*0.762 (0.35λ *0.35λ *0.002λ)	13	4
[8]	> 3 dB in the whole band	3.95-10.6 (2.68:1)	No	1.5-5	Simple	59.94*59.94*1.14 (0.79λ *0.79λ *0.015λ)	1.5	2
[11]	2-6 (3:1)	1.9-8.5 (4.47:1) (VSWR< 2.5)	Yes	-6-7.5	Complex	36*36*20 (0.24λ *0.24λ *0.13λ)	7	2
[19]	2.1-3.1 (1.48:1)	2-19 (9.5:1)	Yes	-6-7	Complex	130*130 (0.9λ *0.9λ)	2	2
[20]	1.5-3 (2:1)	0.8-3 (3.75:1)	Yes	-10-5	Complex	76.2*76.2*38.1 (0.38λ *0.38λ *0.19λ)	7	2
[21]	0.5-1.4 (2.8:1)	0.5-1.4 (2.8:1)	Yes	-5-3.1	Complex	127*127*52 0.21λ *0.21λ *0.09λ)	14	2
This work	0.75-3.64 (4.87:1)	0.29-5 (>17:1)	No	-2-7.1	Simple	105*129*17.5 (0.26λ *0.3λ *0.04λ)	1	2

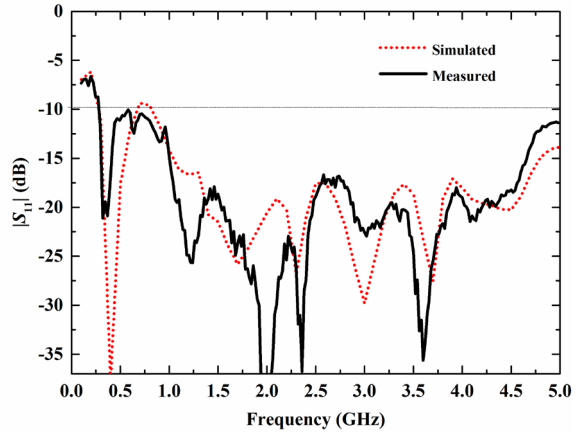

Fig. 11. Simulated and measured $|S_{11}|$ of the proposed antenna.

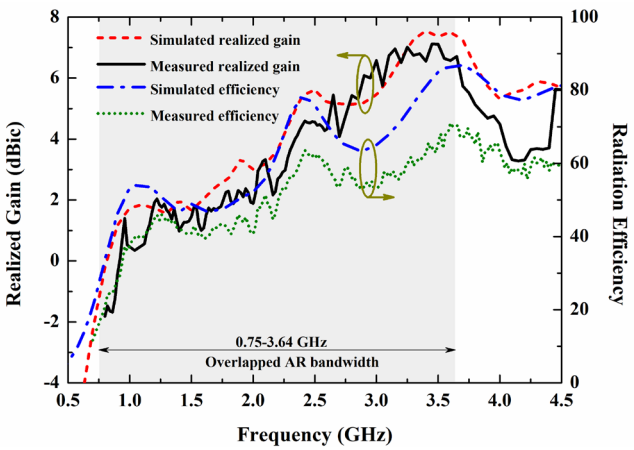

Fig. 12. Simulated and measured realized gains and radiation efficiency of the proposed antenna.

around 71%, while the simulated radiation efficiency can reach 87%. The discrepancy may cause by the measurement errors from both the gain and the directivity. The low efficiency at the low frequency range is mainly attributed to the absorption loss of the embedded RF resistor and the relatively small electrical size.

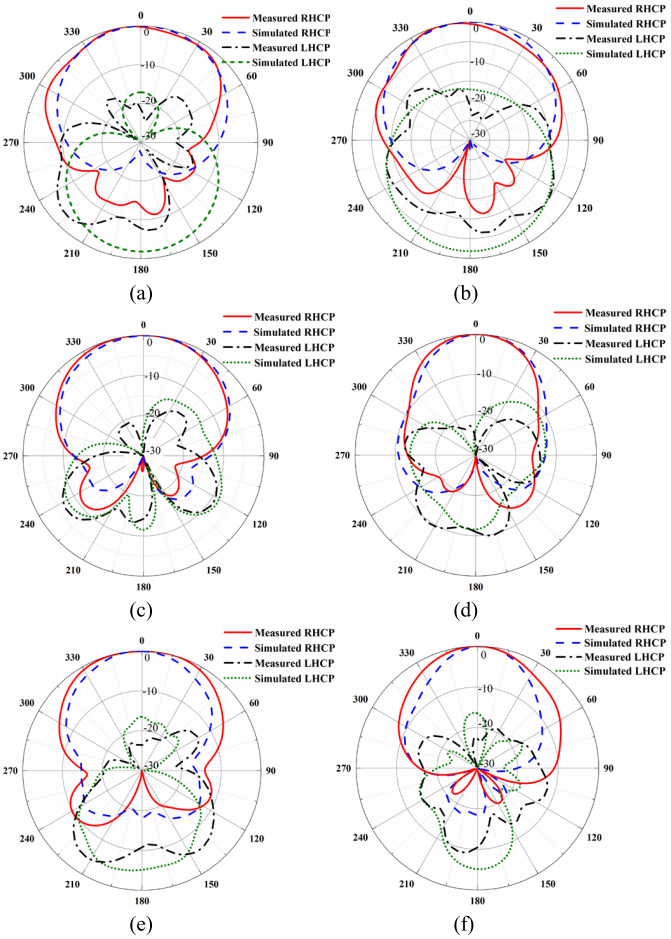

Fig. 13. Measured and simulated normalized radiation patterns of the proposed antenna. (a) 1.2 GHz *xoz* plane. (b) 1.2 GHz *yoz* plane. (c) 2.5 GHz *xoz* plane. (d) 2.5 GHz *yoz* plane. (e) 3.3 GHz *xoz* plane. (f) 3.3 GHz *yoz* plane.

Measured and simulated radiation patterns of the proposed antenna at 1.2, 2.5, and 3.3 GHz are depicted in Fig. 13. It is found that the radiation pattern is not symmetric in the two main planes at 2.5 GHz.

The reason for this phenomenon is that Mode 3 and Mode 1 are stimulated simultaneously at this frequency. The superposition of Mode 3 destructs the pattern symmetry of Mode 1 and yields an asymmetric radiation pattern in the two main planes [17].

Moreover, it is worth noticing that unidirectional radiation pattern with front-to-back ratio (FBR) of 10 dB is achieved at 2.5 GHz without backing any reflectors. But at the low frequency, the FBR is not so good due to the limited size of lower spiral, which leads to inefficient reflection to the downward radiation. To solve this issue, two methods, i.e., adding an additional ground plane and introducing an absorber-filled cavity, are usually employed. An additional ground plane or an absorber-filled cavity can improve the FBR, but the antenna size will be increased significantly. To make spiral antennas flush mountable, absorber-filled cavity is always deployed. However, absorber materials are not suitable for some applications such as airborne antennas due to the thermal and mechanical constraints [18].

To investigate the antenna performance over wide field of view, the AR and wobble on the wave (WoW) are also examined. It is found that the AR is smaller than 3 dB within the elevation angle range of $\pm 30^\circ$ over all phi cuts across the operating band. Moreover, the AR is smaller than 3 dB within the elevation angle range of $\pm 50^\circ$ over all phi cuts at the center frequencies. The WoW is smaller than 1 dB within the range of theta from 0° to 30° except at the high frequencies. The deterioration of the WoW may attribute to the large MSR and the excitation of high-order spiral mode [17].

The antenna performance with a ground plane backed is also investigated. From simulation, it is found that the AR bandwidth will be affected when the distance between the antenna and ground plane (H_g) is smaller than 20 mm. In spite of the reduced AR bandwidth, the proposed antenna still demonstrates much wider bandwidth than the single-turn spiral even with the presence of the ground plane. It is also found that the presence of the ground plane has little influence on the impedance bandwidth, especially when H_g exceeds 10 mm. In addition, the introduction of the ground plane yields a gain increase for the proposed antenna at low frequency range, which makes the antenna gain more stable across the whole operating band.

To demonstrate the excellent performance of the proposed stacked spiral antenna, Table II compares the proposed antenna and other spiral antennas with comparable size. As can be seen from the table, it is obvious that the proposed antenna exhibits simpler feeding configuration, much wider impedance bandwidth ($>$17:1) and AR bandwidth (4.87:1) than other reported work. Moreover, the proposed antenna achieves the superior performance by merely using single-turn arms. Although the radiation efficiency is close to that of the absorber backed spiral antenna [21] at the low-frequency range, the proposed antenna has wider operating bandwidth, higher antenna gain, and lower antenna height. Moreover, the use of the absorber and cavity makes the absorber backed spiral antenna rather bulky and unfavorable for applications where a lightweight and compact design is vital [22].

IV. Conclusion

A single-turn stacked spiral antenna with ultrawide impedance bandwidth, AR bandwidth, and compact size is presented. A tapered planar microstrip line is integrated to feed the spiral antenna, which simplifies the feeding structure. By stacking two orthogonal single-turn spirals and connecting them by metallic posts with proper diameters, the Mode 1 cutoff frequency of the single-turn spiral is decreased significantly. Attributed to the extension of the traveling-wave current path, an ultrawide impedance bandwidth from 0.29 to more than 5 GHz ($>$17:1) and an ultrawide 3 dB AR bandwidth from 0.75 to 3.64 GHz (4.87:1) have been achieved. With its ultrawide bandwidth and compact size, the proposed antenna would be a promising candidate for various applications such as high data-rate satellite communications.

References

[1] D. S. Filipovic and T. P. C. Sr, "Frequency independent antennas," in *Antenna Engineering Handbook*, 4th ed. New York, NY, USA: McGraw-Hill, 2007.

[2] Y. Zhao and W. Hu, "Design of a UWB unidirectional radiation compound spiral antenna," in *Proc. IEEE 6th Int. Symp. Microw., Antenna, Propag., EMC Technol. (MAPE)*, Oct. 2015, pp. 158–161.

[3] I. D. H. Saenz, R. Guinvarcrh, and R. L. Haupt, "Estimating the bandwidth of spiral antenna arrays," *IEEE Antennas Wireless Propag. Lett.*, vol. 15, pp. 1337–1340, 2016.

[4] T.-K. Chen and G. H. Huff, "Stripline-fed Archimedean spiral antenna," *IEEE Antennas Wireless Propag. Lett.*, vol. 10, pp. 346–349, Feb. 2011.

[5] G. H. Huff and T. L. Roach, "Stripline-based spiral antennas with integrated feed structure, impedance transformer, and Dyson-style balun," in *Proc. IEEE Antennas Propag. Soc. Int. Symp.*, Jun. 2007, pp. 2698–2701.

[6] M. A. Elmansouri, J. B. Bargeron, and D. S. Filipovic, "Simply-fed four-arm spiral-helix antenna," *IEEE Trans. Antennas Propag.*, vol. 62, no. 9, pp. 4864–4868, Sep. 2014.

[7] D. Li, L. Li, Z. Li, and G. Ou, "Four-arm spiral antenna fed by tapered transmission line," *IEEE Antennas Wireless Propag. Lett.*, vol. 16, pp. 62–65, Feb. 2017.

[8] T. W. Eubanks and K. Chang, "A compact parallel-plane perpendicular-current feed for a modified equiangular spiral antenna," *IEEE Trans. Antennas Propag.*, vol. 58, no. 7, pp. 2193–2202, Jul. 2010.

[9] K. Louertani, R. Guinvarc'h, N. Ribiere-Tharaud, and M. Helier, "Multiarms multiports externally fed spiral antenna," *IEEE Antennas Wireless Propag. Lett.*, vol. 11, pp. 236–239, 2012.

[10] I. Hinostroza, R. Guinvarc'h, and R. L. Haupt, "Two stacked orthogonally wound spirals with connected arms," in *Proc. IEEE Int. Symp. Antennas Propag., USNC/URSI Nat. Radio Sci. Meeting*, Jul. 2015, pp. 1976–1977.

[11] Y.-W. Zhong, G.-M. Yang, J.-Y. Mo, and L.-R. Zheng, "Compact circularly polarized Archimedean spiral antenna for ultrawideband communication applications," *IEEE Antennas Wireless Propag. Lett.*, vol. 16, pp. 129–132, Mar. 2017.

[12] M. Veysi and M. Kamyab, "Bandwidth enhancement of low-profile PEC-backed equiangular spiral antennas incorporating metallic posts," *IEEE Trans. Antennas Propag.*, vol. 59, no. 11, pp. 4315–4318, Nov. 2011.

[13] I. D. H. Saenz, R. Guinvarch, R. L. Haupt, and K. Louertani, "A 6:1 bandwidth, low-profile, dual-polarized ring array of spiral antennas with connecting arms," *IEEE Trans. Antennas Propag.*, vol. 64, no. 2, pp. 752–756, Feb. 2016.

[14] M. A. Amiri, C. A. Balanis, and C. R. Birtcher, "Gain and bandwidth enhancement of a spiral antenna using a circularly symmetric HIS," *IEEE Antennas Wireless Propag. Lett.*, vol. 16, pp. 1080–1083, 2017.

[15] J. Kaiser, "The Archimedean two-wire spiral antenna," *IRE Trans. Antennas Propag.*, vol. 8, no. 3, pp. 312–323, May 1960.

[16] T.-K. Chen and G. H. Huff, "On the constant input impedance of the Archimedean spiral antenna in free-space," *IEEE Trans. Antennas Propag.*, vol. 62, no. 7, pp. 3869–3872, Jul. 2014.

[17] H. Nakano, H. Mimnaki, J. Yamauchi, and K. Hirose, "A low profile Archimedean spiral antenna," in *Proc. IEEE Antennas Propag. Soc. Int. Symp.*, Jun./Jul. 1993, pp. 450–453.

[18] L. Schreider, X. Begaud, M. Soiron, and B. Perpere, "Archimedean microstrip spiral antenna loaded by chip resistors inside substrate," in *Proc. IEEE Antennas Propag. Soc. Symp.*, Jun. 2004, pp. 1066–1069.

[19] W. Fu, E. R. Lopez, W. S. T. Rowe, and K. Ghorbani, "A planar dual-arm equiangular spiral antenna," *IEEE Trans. Antennas Propag.*, vol. 58, no. 5, pp. 1775–1779, May 2010.

[20] J. M. O'Brien, J. E. Grandfield, G. Mumcu, and T. M. Weller, "Miniaturization of a spiral antenna using periodic Z-plane meandering," *IEEE Trans. Antennas Propag.*, vol. 63, no. 4, pp. 1843–1848, Apr. 2015.

[21] T.-Y. Shih and N. Behdad, "A compact, broadband spiral antenna with unidirectional circularly polarized radiation patterns," *IEEE Trans. Antennas Propag.*, vol. 63, no. 6, pp. 2776–2781, Jun. 2015.

[22] M. C. Buck and D. S. Filipovic, "Spiral cavity backing effects on pattern symmetry and modal contamination," *IEEE Antennas Wireless Propag. Lett.*, vol. 5, pp. 243–246, 2006.